Research Article

Blast mitigation by perforated plates using an explosive driven shock tube: study of geometry effects and plate numbers

T. Schunck[1] · D. Eckenfels[1]

© The Author(s) 2021   OPEN

Abstract

This work is set in the context of blast mitigation based on geometric means, namely perforated metallic plates or grids. When a shock wave passes through a perforated plate, the flow field is modified, and new shock waves are created, as well as regions of vortices and turbulence in which the energy of the wave can be dissipated. In this study, an explosive driven shock tube (EDST) was used to visualize the interaction of a blast wave with perforated plates or with a piece of cast metallic foam. Additionally, the overpressure and the impulse of the reflected blast wave on a wall located downstream were assessed. The use of an EDST allowed the evaluation of the mitigation capacity under a high dynamic loading. Several combinations of perforated plates were tested, varying the geometry and the number of plates, as well as switching between two different spacings. When the shock wave collided with a plate, we observed that part of the incident shock wave was reflected by the plate, while the remaining wave was transmitted through it. Downstream of the plate, both the overpressure and the impulse were reduced, this effect being more prominent as the porosity of the plates decreased. When two plates were placed as obstacles, this phenomenon of reflection/transmission was repeated twice consecutively, further reducing the downstream reflected overpressure and impulse. An array of three plates or a piece of metallic foam were even more effective in mitigating the blast wave. Varying the distance between two or three plates had no effect on blast mitigation.

Article highlights

- Assessment of the blast mitigation capacity of perforated plates.
- Assessment of the effect of geometry, number of plates and spacing.
- Visualization of the propagation and the interaction of the shock wave with the perforated plates.

1 Introduction

Shock tubes have been extensively used to assess high speed aerodynamics and shock wave parameters, but also the response of materials to blast loading. There exist two main categories based on how the shock wave is created: compression-driven (conventional) or explosive-driven. Shock tubes come in a broad range of shapes, and can therefore produce various shock waves profiles. In a conventional shock tube, the shock wave typically has a thickness of a few mean free paths, and, in an ideal case, the compressed gas reaches its equilibrium values of pressure,

density, and temperature within this distance. However, modifications could be carried out on compression-driven shock tubes in order to generate a blast shock wave and to obtain a Friedlander-type wave (characterized by a pressure jump followed by progressive decay) at a specific location in the tube. The shock tube is designed so that the reflection of expansion waves on the driver end can combine with the incident wave, and the pressure signal in the tube at a certain distance from the membranes is similar to a blast shock wave. An explosive-driven shock tube (EDST) is a simple tube where a given high explosive charge is placed near one end and detonated. The blast wave is directed out of the opposite open end by the tube, producing a realistic blast profile. The EDST is a good alternative for studies conducted at small-scale with high pressure shock waves. High overpressures can be obtained with small charges, and optical measurements are possible thanks to the lack of fireball. The repeatability and the reproducibility are improved. However, only a rather small area of the sample can be subjected to the blast wave. Furthermore, the load being uniform on the surface of the sample, it is only representative for long range charge detonation. EDST is an efficient blast loading tool for the study of new protective techniques. The protection of buildings and people against highly dynamic loadings caused by explosions is a major concern since the number of terrorist attacks on civilian and military infrastructure continue to rise all over the world. Various techniques have been developed to absorb, disrupt and ultimately reduce the effect of a blast wave before it reaches its intended target. These techniques are broadly classified as either active or passive.

Active mitigation techniques need to be actively deployed in response to a blast threat or a blast event. At first, the threat or explosion must be detected, then the mitigation system is activated. An example of an active blast mitigation system could be a water deluge system used on an offshore oil or gas platform in case of a gas cloud [1]. A water mist system in an infrastructure [2] is another example. These systems are not generally activated by the detonation. Instead, they are activated preventively if there is an imminent risk of detonation. Passive systems are embedded within the structural design and don't require to be triggered. They include protective sacrificial cladding, geometrical arrangements, granular filters and perforated plates. Sacrificial cladding is a blast mitigation technique based on the behaviour of cellular materials under compression [3]. Geometrical arrangements can be used to deflect the blast wave. Berger et al. [4] have investigated the effect of obstacles on the shock-wave load developed at the centre of the end-wall of a shock tube. Granular filters and perforated plates are designed to disrupt the blast wave. Granular filters are widely used as protectors against shock waves. Ben-Dor et al. [5] have studied the pressure fields in front of and inside granular layers during their interaction with weak shock waves. Their performance as a function of different parameters, such as the filter's length, diameter, and density of beads, has been assessed [6]. The description of the interaction of a shock wave with grid-like obstacles started in the 1950s [7]. It has been shown that grids or perforated plates modify the flow field by introducing new shock waves, regions of vortices, and considerable turbulence in which the energy of the incident shock wave can be dissipated. Thereafter, several studies discussing the attenuation of a shock wave passing through a perforated plate were achieved with a shock tube [8–11]. In [12], a transonic shock tube was used to visualize the interaction of a blast wave profile with a metallic perforated plate and three types of grid with different porosities were tested. The highest attenuation was obtained with the grid having the lowest porosity. Langdon et al. [13] have observed the mitigation capacity of perforated plates on plates fully clamped to blast loading directed down a tube. The influence of a mild steel plate's thickness and hole size on its response to blast loading has been also studied [14]. It was observed that only the plates with the smallest hole size effectively reduced the mid-point deflection while increasing the tearing threshold impulse. Recently, the shock wave attenuation performance of protective barriers made of metal ring mesh or perforated plates were also investigated [12, 15, 16]. The use of perforated plates seems to be of interest for protection purposes but still needs some further work and improvement. The use of a configuration with several plates could represent an option of improvement. Indeed, it has been shown that shock wave trapping between two perforated plates enhanced the shock wave attenuation downstream from the grids [17].

The purpose of the present work is to introduce an experimental setup which is of particular interest for the study of blast mitigation passive systems. Indeed, it will allow the visualization of the shock wave's interaction with the blast mitigating system as well as the estimation of the latter's mitigation efficiency. In fact, it combines an EDST with a retroreflective shadowgraph imaging technique. This setup was used to assess the blast mitigation capacity of perforated plates. The EDST generates stronger blast waves compared to conventional shock tubes. Consequently, the mitigation capacity of the perforated plate or array of several plates can be assessed under a load comparable to that produced by several kilograms of high explosive detonated at several meters from a target. High-speed imaging was realized, and the interaction of the blast wave with the metallic plates was visualized. The effect of the perforated plates on the reflected overpressure was measured on a wall placed behind the setup.

Several geometries of perforated plates were tested as well as different numbers of plates and two spacings. A slice of cast metallic foam was also tested. The phenomenon of blast interaction with perforated plates as well as the mitigation capacity will be compared with data obtained with conventional shock tubes at weak shock waves. The motivation and objectives of this study are given in this introduction (Sect. 1). The experimental setup is described in Sect. 2. The experimental data are presented in Sect. 3 and discussed in Sect. 4. Conclusions along with some remarks concerning the experimental setup and shock wave attenuation performance of perforated plates are summarized in Sect. 4.

2 Materials and methods

2.1 Explosive driven shock tube (EDST)

The EDST was based on previously published works [18, 19]. The shock tube has a square 100 mm × 100 mm external and 80 mm × 80 mm internal section, with a total length of 1750 mm (Fig. 1). A pressure sensor (Kulite HKS 375) is used to measure the reflected overpressure on a wall behind the plates. Spherical charges of C4 were used ($m = 15$ g) to produce a planar blast wave. All the charges were cast and detonated without any container at 50 mm from the shock tube inlet (Fig. 1).

The distance between the outlet of the EDST and the wall was 180 mm. The plate, or the last plate in case of several plates, was positioned 50 mm in front of the wall. The spacing between the plates was either 25 or 40 mm. The number of plates serving as porous barriers was either one, two or three. The position of the plates for each configuration tested is given in Fig. 2.

2.2 Samples

Three types of perforated plate were tested. The first one is a metallic plate with small round holes, the second one has large round holes and the third one has square holes (Fig. 3). Plates made of expanded metal were also investigated (Fig. 4A). Expanded metal is a metal sheet that has been cut and stretched to form a regular pattern. It is stronger than an equivalent weight of wire mesh because the material is flattened, allowing the metal to stay in one piece. The expanded metal used in the present study had a hexagonal mesh. A slice of casted metallic foam (F.T.B) was also tested (Fig. 4B). The foam had a cell size of 30 mm with holes of 12 and 5 mm in diameter. The characteristics of the perforated plates and of the expanded metal are given in Table 1.
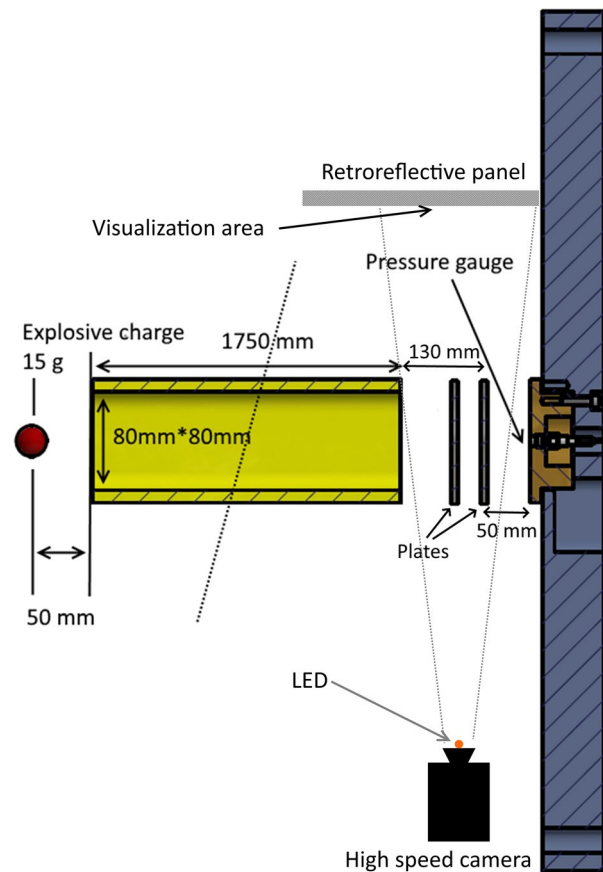

Fig. 1 Schematic view of the explosive-driven shock tube and positioning of the pressure sensor and plates

2.3 Imaging

A high-speed Photron SA-Z camera was used to record images of the propagation and the interaction of the shock wave with the plates, or the cast metallic foam, using a retroreflective shadowgraph technique [20]. An Extreme High Power Light Emitting Diode (LED) (XHP70.2, CREE), located on an axis shared with the centre of the camera lens, illuminated the outlet of the EDST as well as a panel covered by a retroreflective material (3 M Reflex-folie 4090), which was placed in the background (Fig. 1). A power supply and a purposely built trigger unit allowed the LED to be pulsed for about 10 ms. The reflection and the transmission patterns of the shock wave through the obstacle could be visualized via their shadow on the panel which was imaged by the camera. Figure 5 shows a photograph of the camera with the LED and the EDST (Fig. 5A) and the details of the fixing system of the samples (Fig. 5B). In the background, the retroreflective panel is observable (Fig. 5B). The videos were recorded with a frame rate of 10^5 fps at a resolution of 408 × 384 pixels. The exposure time ranged from 7 to 8 μs.

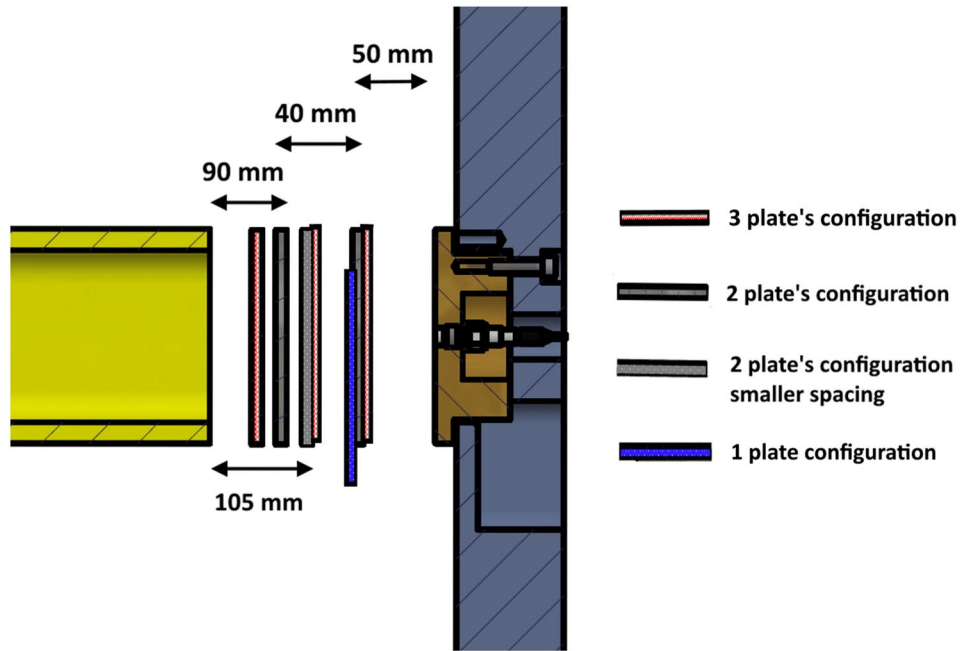**Fig. 2** Position of the plates for each configuration tested

Fig. 3 Metal grids. **A** Small round holes, porosity of 48%, hole size of 10 mm and distance of 14 mm between the holes, thickness of 1.5 mm; **B** large round holes, porosity of 49.8%, hole size of 20 mm and distance of 27 mm between the holes, thickness of 2 mm; **C** square holes, porosity of 69.4%, hole size of 10 mm and distance of 12 mm between the holes, thickness of 1.5 mm
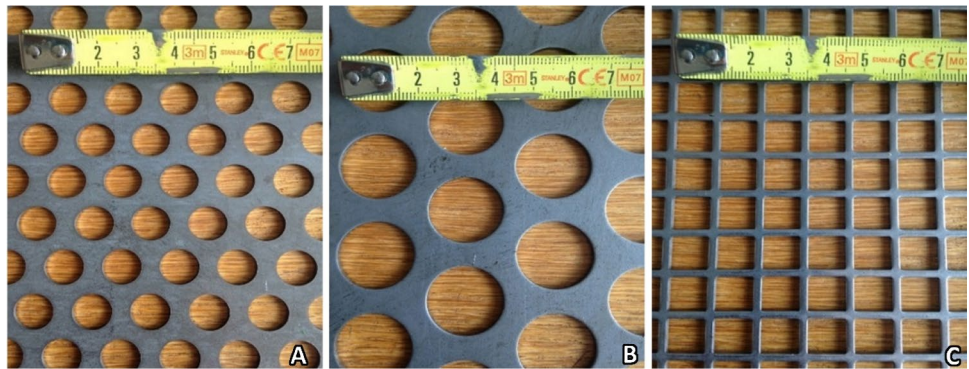

Fig. 4 **A** Plate of expanded metal, open area of 24%, hole size of 45 mm * 13 mm, thickness of 3 mm, apparent thickness of 9 mm, strand of 5 mm; **B** piece of cast metallic foam, cell size of 30 mm with holes of 12 and 5 mm diameter
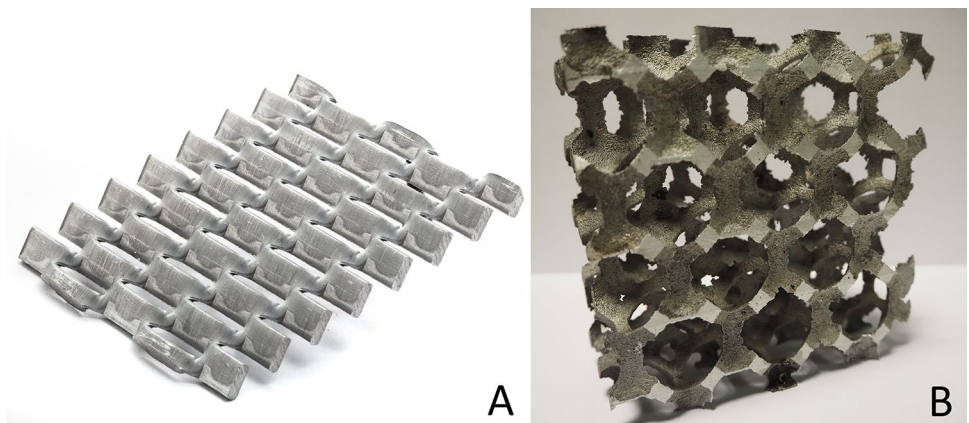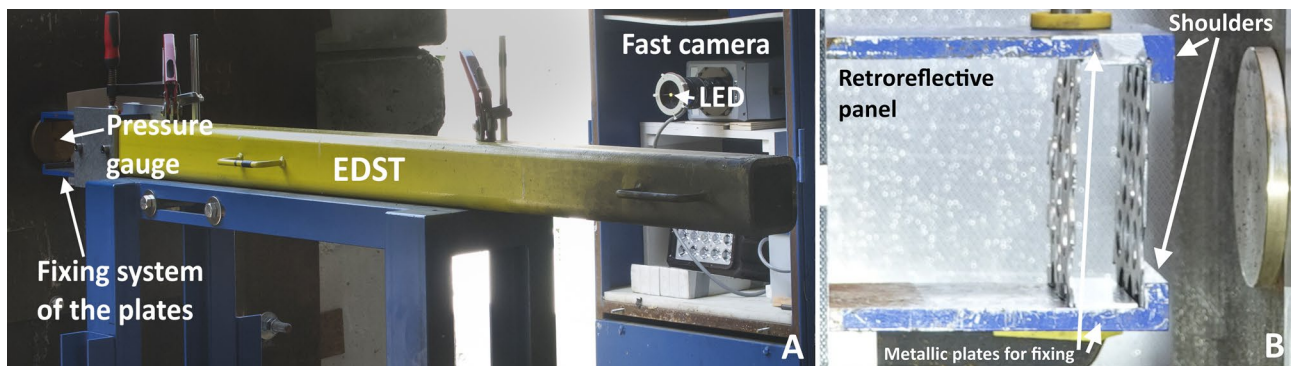
Table 1 Characteristics of the perforated plates and of the expanded metal

	Small round holes	Large round holes	Square holes	Expanded metal
Porosity (%)	48	49.8	69.4	24
Hole size (mm)	10	20	10	–
Thickness (mm)	1.5	2	1.5	3
Distance between the holes (mm)	14	27	12	–
Pitch pattern x/y				45/13
Strand (mm)	–	–	–	5
Apparent thickness (mm)	–	–	–	9

Fig. 5 **A** Experimental setup showing the explosive driven shock tube and the fast camera with the LED. **B** Detail of the metallic plates used for the fixing of the samples

3 Results

3.1 Imaging

Figure 6 shows the shock wave propagating at the outlet of the EDST when there was no perforated plate. The photographs were taken with fast imaging. The shock wave was not totally plane at the outlet of the tube due to the mounting system of the perforated plates. Indeed, two metallic plates were fixed parallel to the EDST at the end, and the shock wave was reflected by these two plates. The two plates had a shoulder at the end which provided additional thrust for the fixation of the perforated plates. These shoulders can be seen in Fig. 5. From $t = 1470$ μs, the shock wave reflection on them was also visible. The reflection of the shock wave on the wall, where the pressure gauge was inserted, was observable from $t = 1540$ μs.

Figure 7 shows the shock wave propagation through one metallic plate with square holes. The plate was positioned at a distance of 130 mm from the tube outlet and at a distance of 50 mm in front of the wall. When passing through the holes ($t = 1540$ μs), the shock wave split into several shock waves ($t = 1550$ μs), one for each hole,

and these shock waves recombined further down. At $t = 1570$ μs, the shock wave behind the perforated plate was almost plane. A complex structure of turbulence just behind the grid was visible and lasted for a long time. At $t = 1560$ μs turbulence began to form behind the grid, and was still observable at $t = 1790$ μs. Moreover, it was still very marked at over 240 μs and over a distance of 1 cm, until the arrival of the wave reflected by the wall made them disappear. The shock wave that had passed through the perforated plate was reflected by the wall at $t = 1630$ μs. The remaining shock wave, which did not pass through the grid, was reflected by the grid. This led to the pattern formed at the back of the grid ($t = 1550$ μs). In the same way, the reflected shock waves recombined further down, and at about $t = 1570$ μs, the resulting wave was almost plane.

Figure 8 shows the shock wave propagation through two metallic plates with small round holes. The first plate was positioned at a distance of 90 mm from the tube outlet and at a distance of 90 mm in front of the wall. The two grids were 40 mm apart. When passing through the holes of the first plate ($t = 1440$ μs), the shock wave split into several shock waves, one for each hole, which then recombined further down. The transmitted shock wave
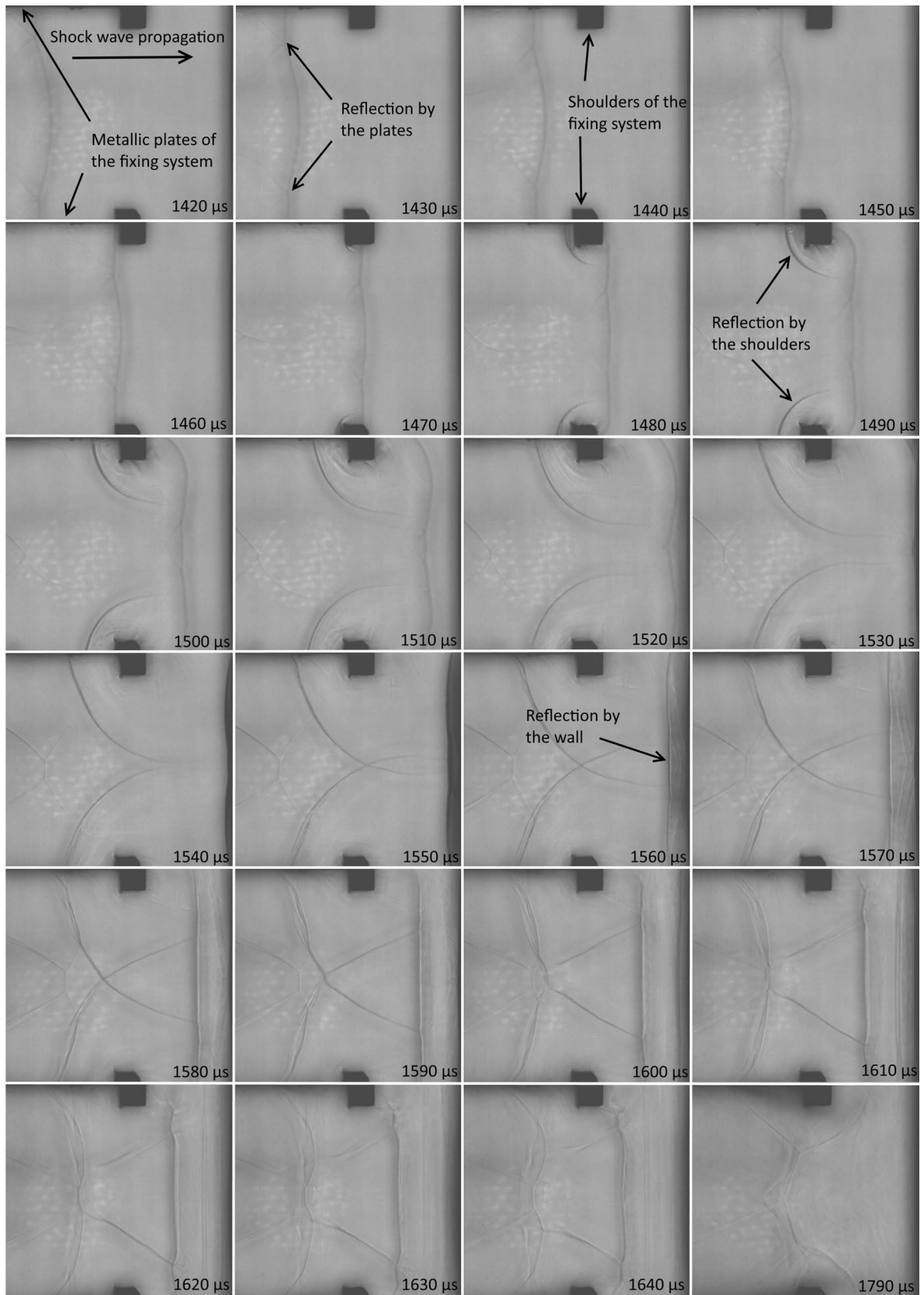
Fig. 6 Photographs resulting from fast video recording, showing the shock wave propagation at the outlet of the EDST (10 μs between each photograph)
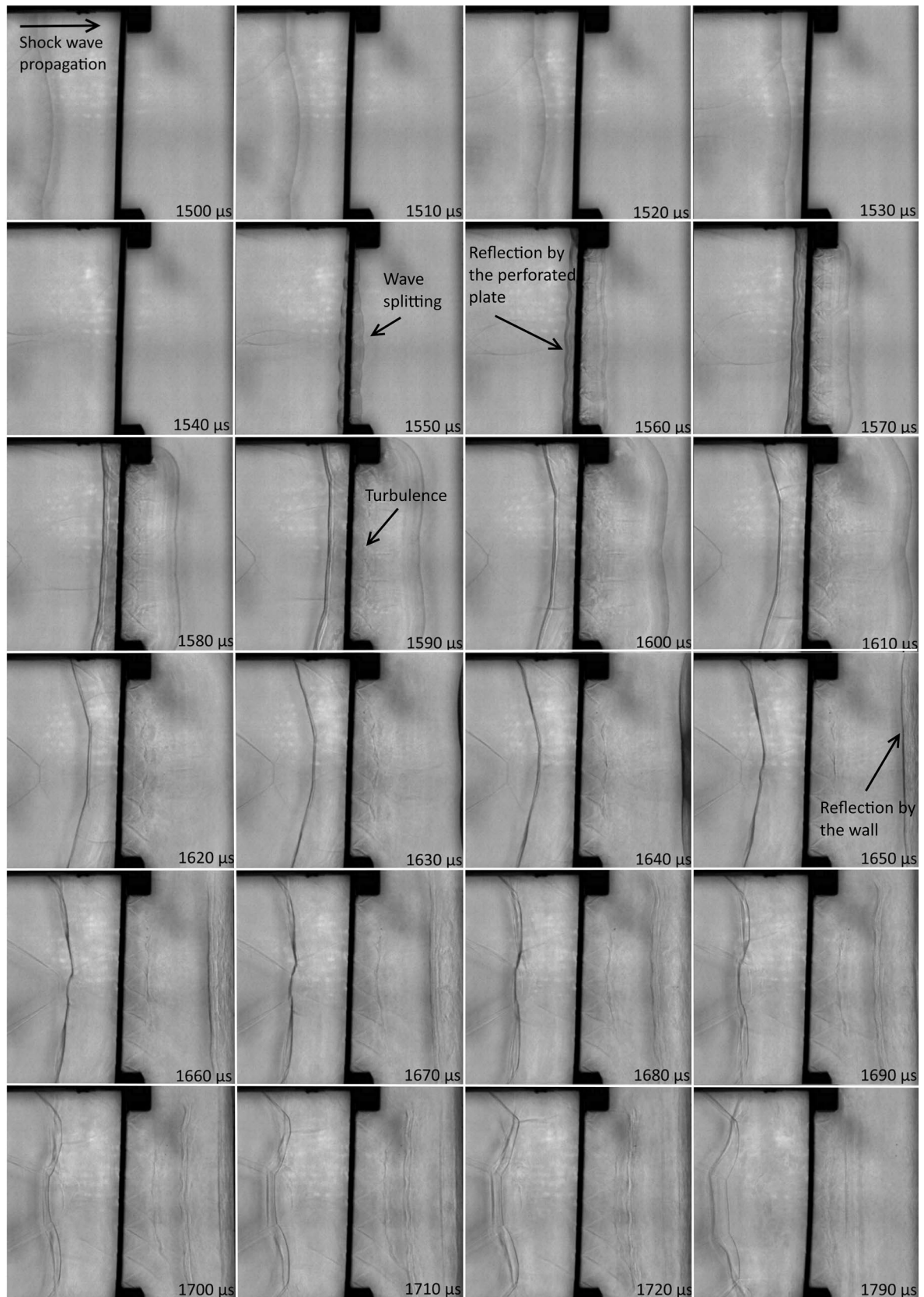
Fig. 7 Photographs resulting from fast video recording, showing the shock wave propagation through the perforated plate with square holes (10 µs between each photograph)
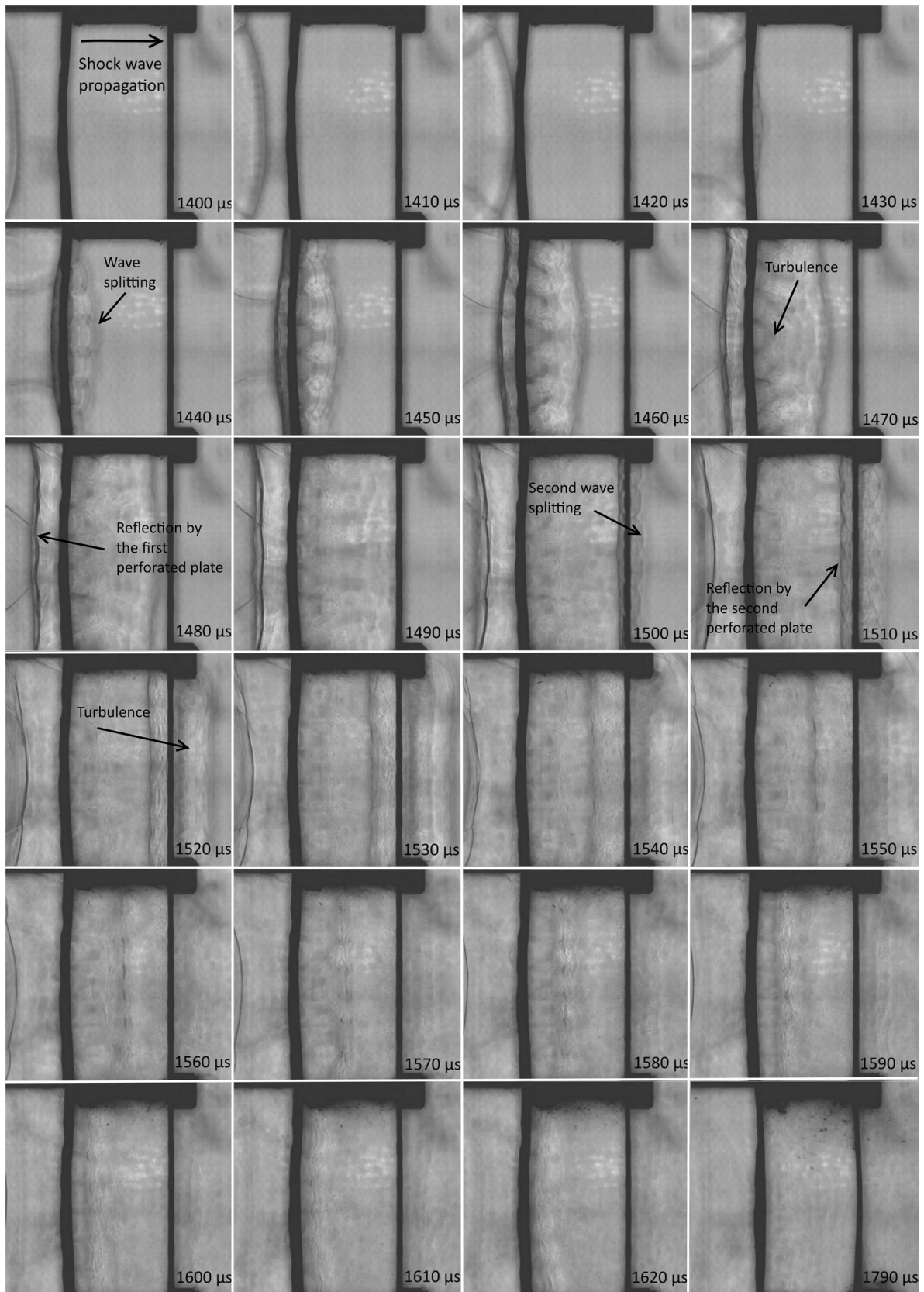
Fig. 8 Photographs resulting from fast video recording, showing the shock wave propagation through the two perforated plates having small round holes (10 μs between each photograph)

resembled the incident shock wave at $t = 1460$ μs. At the back of the shock wave, between the two plates, lasting turbulence can be observed, especially just behind the plate. The remaining shock wave, which did not pass through the first plate, was reflected and led to the pattern at the back of this plate. Thereafter, the shock wave transmitted by the first perforated plate impacted the second plate ($t = 1490$ μs) and, once again, a part of the shock wave was transmitted, and another part was reflected. The wave reflected by the second plate propagated towards the first plate and, as it arrived near the plate, the shock front and the turbulence became less obvious. Turbulence behind the second plate is also visible. The reflection of the transmitted shock wave on the wall, where the pressure gauge was inserted, was not clearly observable.

Figure 9 shows the shock wave propagation through the slice of cast metallic foam. When the shock wave impacted the foam ($t = 1550$ μs), a part of the shock wave passed through the foam holes. The remaining shock wave, which did not pass through, was reflected by the foam and led to the pattern at the back of the foam slice ($t = 1560$ μs). At $t = 1630$ μs, at the back of the foam, the reflected shock wave was almost plane. After 80 μs, the shock wave emerged from the foam, and the shock front was not very marked.

3.2 Overpressure and impulse profiles

Five reference tests were conducted without any plate, and three to six experiments were conducted with one grid positioned at the outlet of the EDST, varying between each type of plates. The reflected overpressure-time history was collected by the sensor inserted in the wall 50 mm behind the plate, while the plate was located 130 mm in front of the EDST. The impulse-time history was also computed. The impulse is defined as the overpressure signal integrated over time. Figure 10A compares the reflected overpressure-time histories between a reference test with no plate and the tests with various kind of plates or with the cast metallic foam. The impulse-time histories are plotted on Fig. 10B. The maximum reflected overpressures for all the tests are listed in Table 2, and the maximum reflected impulses are given in Table 3. The attenuation of the maximum reflected overpressure or of the maximum reflected impulse, compared to the mean value obtained in the reference tests, are also given in Tables 2 and 3, respectively.

The maximum reflected overpressure on the wall was reduced by about 30–40% for the plates with round holes and the expanded metal plate. The attenuation was only about 23% for the plate with square holes whereas the piece of cast metallic foam induced a strong decrease of about 66–73%. The maximum reflected impulse was reduced by about 60–65% for the plates with round holes

and the expanded metal plate, and by about 85% for the cast metallic foam. The impulse reduction was about 46% for the plate with square holes.

Figure 11A shows the time history of reflected overpressure obtained in a reference test without plate and in tests combining two identical plates. The two plates were 40 mm apart and the second plate was located 50 mm in front of the wall with the pressure gauge. The first plate was positioned at a distance of 90 mm from the tube outlet and at a distance of 90 mm in front of the wall. The result obtained for the cast metallic foam is also plotted. Figure 11B shows the impulse versus time for the same experiments. Three or four experiments were conducted with two plates positioned at the EDST's outlet for each geometry of plate. The maximum reflected overpressure on the wall was reduced by about 30% when two plates with square holes were positioned in front of the EDST (Table 2). This reduction is slightly higher to that obtained with one plate. The use of two plates with round holes or out of expanded metal enhanced the reflected overpressure mitigation. The maximum reflected overpressure decrease was about 50–60% for the perforated plates and up to 70% for the expanded metal (Table 2). The mitigation obtained with two plates of expanded metal approximated that obtained with the piece of cast metallic foam (Table 2). The maximum reflected impulse was reduced by about 82–85% for the plates with round holes and by about 89% for the two expanded metal plates (Table 3). The impulse reduction was about 63% for the plate with square holes, which is slightly more than those obtained with one plate.

The effect of the spacing between two plates on the blast mitigation has been assessed. In addition, two experiments involving two plates of each geometry were conducted. The plates were separated by 25 mm, positioned at the outlet of the EDST. The second plate was located 50 mm in front of the wall with the pressure gauge, and consequently the first plate was located 105 mm in front of the EDST. Figure 12A presents the reflected overpressure as a function of time obtained in a reference test and in two tests, one with two plates separated by 25 mm, and the other by 40 mm, repeated for each type of plate. Figure 12B presents the impulse for the same experiments. The spacing between the perforated plates had no effect on the reduction of the maximum reflected overpressure or impulse. Indeed, the reduction of the maximum reflected overpressure and of the maximum reflected impulse was similar for the two spacings regardless the type of plate (Tables 2, 3).

In addition, in order to properly assess the effect of the number of plates on blast mitigation, three experiments with three plates of expanded metal positioned at the outlet of the EDST were realised. In the experiments with one
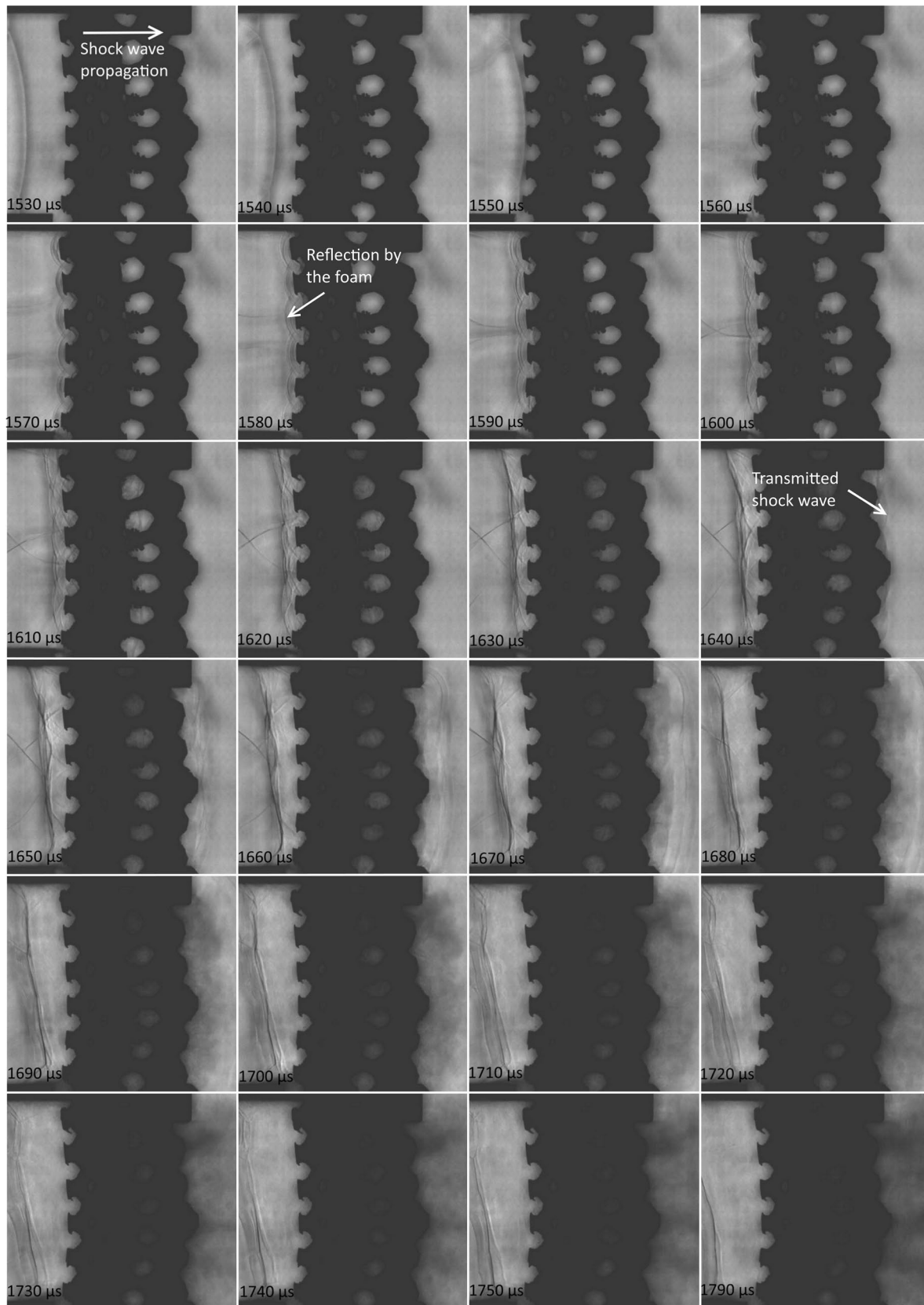
Fig. 9 Photographs resulting from fast video recording, showing the shock wave propagation through a slice of cast metallic foam
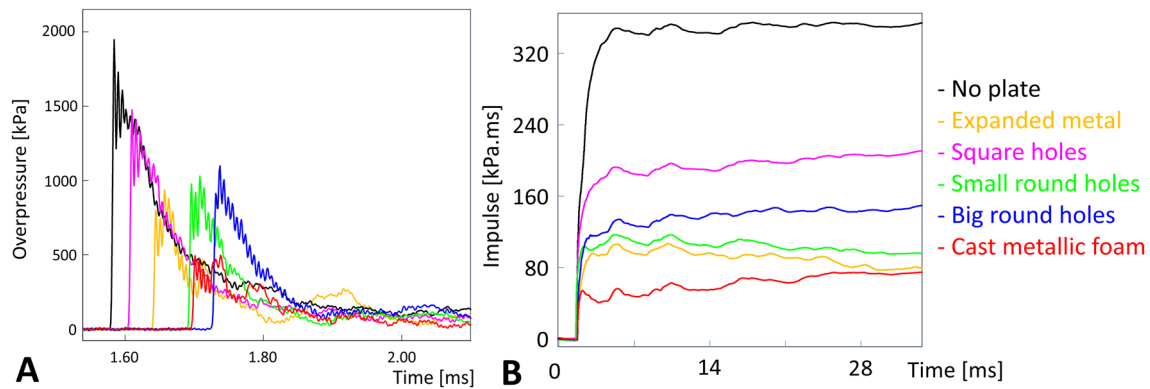
Fig. 10 Reflected overpressure (**A**) and impulse (**B**) measured on the wall positioned 50 mm behind the plate for all types of plate. The figure also shows the results of a reference test, which was performed without plate, as well as the results obtained with the cast metallic foam

plate, the plate was positioned at a distance of 130 mm from the tube outlet and at a distance of 50 mm in front of the wall. In the experiments with two plates, the first plate was positioned at a distance of 90 mm from the tube outlet and at a distance of 90 mm in front of the wall. The two grids were 40 mm apart. The three plates were 25 mm apart, and the third plate was located 50 mm in front of the wall with the pressure gauge. Figure 13A shows the reflected overpressure as a function of time obtained in a reference test without plate and in tests achieved either with one, two or three expanded metal plates. The reduction of the maximum reflected overpressure increased with the number of plates. The maximum reflected overpressure on the wall was reduced by 46, 72 and 84% when one, two and three plates were positioned in front of the EDST, respectively (Table 2). In the same way, the maximum impulse was reduced by 68, 89 and 93% (Table 3).

The relationship between the attenuation of the maximum reflected overpressure, or of the maximum reflected impulse, and the porosity of the obstacle was assessed. In order to take into account the porosity of the plates and the number of plates, a porosity index was defined as P the porosity divided by N the number of plates. The attenuation of the maximum reflected overpressure and of the maximum reflected impulse as a function of the porosity index is depicted in Fig. 14 in a logarithmic scale for all the experiments (except the cast metallic foam). Both attenuations decreased in a logarithmic trend with the porosity index.

3.3 Structural damages of the plates after testing

The plates with small round and square holes had a thickness of 1.5 mm. When one single sample was tested, the plates were distorted. They presented a straight fold in the middle as they were clamped by the mounting system

on two opposite sides. The plates with large round holes were thicker (2 mm), and hence less distorted, and the expanded metal plates were almost not deformed. When an array of two plates was tested, only the first plate was distorted when the plate was relatively thin (small round and square holes). Pieces of cast metallic foam were intact after test.

4 Discussion

The implementation of a retroreflective shadowgraph technique with high-speed imaging in the EDST experiments has shown that when a shock wave collides with a perforated plate, a part of the incident shock wave is reflected by the plate and the remaining part is transmitted through the plate. A rather long time turbulence is observed behind the plate. In the same way, when a shock wave collides with an array of two perforated plates, a part of the incident shock wave is reflected by the first plate and the remaining part is transmitted through the first plate before being reflected by the second plate. A part of the remaining shock wave is even transmitted through the second plate. Turbulence behind the second plate is also observed. The same observations were made by Ram et al. [21] who assessed the propagation of shock waves through an array of perforated plates in a conventional shock tube. Consequently, blast interaction phenomenon with perforated plates at high loading is similar to what occurs at low loading. As expected, the overpressure and the impulse downstream of a perforated plate are reduced, and the reduction increases with decreasing porosity. Indeed, the plate with square holes had only a minor impact on the overpressure and on the impulse. This is probably due to the high percentage of void within the grid (69.4%), causing a larger extent of the shock wave

Table 2 Initial reflected overpressure measured by the sensor inserted in the wall located 50 mm downstream from the porous barriers for all experiments

Type of plate	Number of plates	Spacing (cm)	Overpressure (kPa)	Attenuation (%)
No plate	–	–	2282	–
No plate	–	–	1948	–
No plate	–	–	1561	–
No plate	–	–	1565	–
No plate	–	–	1573	–
Cast metallic foam	1	–	494	72
Cast metallic foam	1	–	622	66
Cast metallic foam	1	–	513	73
Square holes	1	–	1135	36
Square holes	1	–	1475	17
Square holes	1	–	1460	18
Square holes	1	–	1232	31
Square holes	1	–	1579	12
Square holes	1	–	1498	17
Large round holes	1	–	1112	38
Large round holes	1	–	1519	15
Large round holes	1	–	1097	39
Small round holes	1	–	1371	23
Small round holes	1	–	1212	32
Small round holes	1	–	1030	42
Expanded metal	1	–	936	48
Expanded metal	1	–	771	57
Expanded metal	1	–	1089	39
Expanded metal	1	–	1030	42
Square holes	2	4	1056	41
Square holes	2	4	1705	5
Square holes	2	4	1196	34
Square holes	2	4	1102	39
Large round holes	2	4	1365	24
Large round holes	2	4	889	50
Large round holes	2	4	844	53
Large round holes	2	4	814	54
Small round holes	2	4	713	60
Small round holes	2	4	784	56
Small round holes	2	4	670	62
Expanded metal	2	4	446	75
Expanded metal	2	4	450	75
Expanded metal	2	4	586	67
Square holes	2	2.5	995	44
Square holes	2	2.5	1250	30
Large round holes	2	2.5	979	45
Large round holes	2	2.5	1183	34
Small round holes	2	2	659	63
Small round holes	2	2.5	974	45
Expanded metal	3	2.5	325	82
Expanded metal	3	2.5	253	86
Expanded metal	3	2.5	279	84

The difference with the mean value obtained with the reference tests (no plate) is also given

Table 3 Maximum impulse obtained with the sensor inserted in the wall located 50 mm downstream from the porous barriers for all the experiments

Type of plate	Number of plates	Spacing (cm)	Impulse (kPa.ms)	Attenuation (%)
No plate	–	–	320	–
No plate	–	–	400	–
No plate	–	–	350	–
No plate	–	–	370	–
No plate	–	–	340	–
Cast metallic foam	1	–	60	85
Cast metallic foam	1	–	50	85
Cast metallic foam	1	–	60	85
Square holes	1	–	160	55
Square holes	1	–	190	46
Square holes	1	–	200	44
Square holes	1	–	200	43
Square holes	1	–	180	51
Square holes	1	–	226	37
Large round holes	1	–	130	63
Large round holes	1	–	150	57
Large round holes	1	–	130	62
Small round holes	1	–	120	67
Small round holes	1	–	140	62
Small round holes	1	–	110	68
Expanded metal	1	–	110	70
Expanded metal	1	–	120	65
Expanded metal	1	–	130	63
Expanded metal	1	–	150	59
Square holes	2	4	160	55
Square holes	2	4	120	67
Square holes	2	4	124	65
Square holes	2	4	116	68
Large round holes	2	4	60	83
Large round holes	2	4	60	83
Large round holes	2	4	50	85
Large round holes	2	4	90	76
Small round holes	2	4	50	86
Small round holes	2	4	60	83
Small round holes	2	4	50	87
Expanded metal	2	4	30	93
Expanded metal	2	4	50	87
Expanded metal	2	4	50	87
Square holes	2	2.5	120	67
Square holes	2	2.5	140	61
Large round holes	2	2.5	70	80
Large round holes	2	2.5	120	66
Small round holes	2	2	50	87
Small round holes	2	2.5	70	79
Expanded metal	3	2.5	30	93
Expanded metal	3	2.5	20	93
Expanded metal	3	2.5	30	93

The difference with the mean value obtained with the reference tests (no plate) is also given
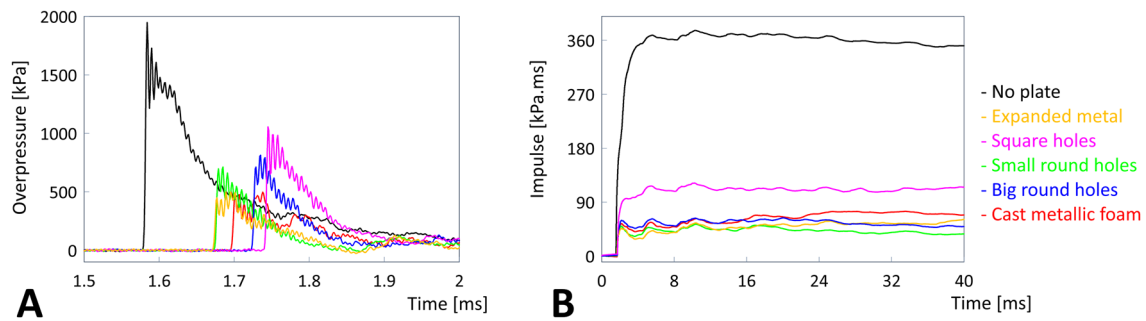
Fig. 11 Reflected overpressure (**A**) and impulse (**B**) measured on the wall positioned 50 mm behind the two plates for all types of plate. The figure also shows the results of a reference test, which was performed without plates, as well as the results obtained with the cast metallic foam
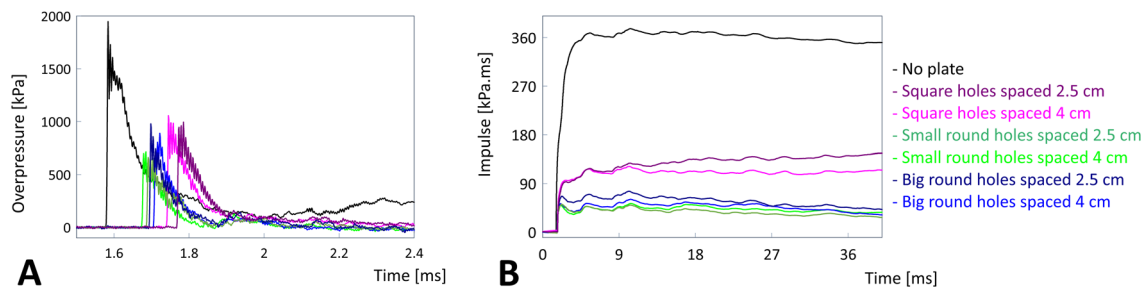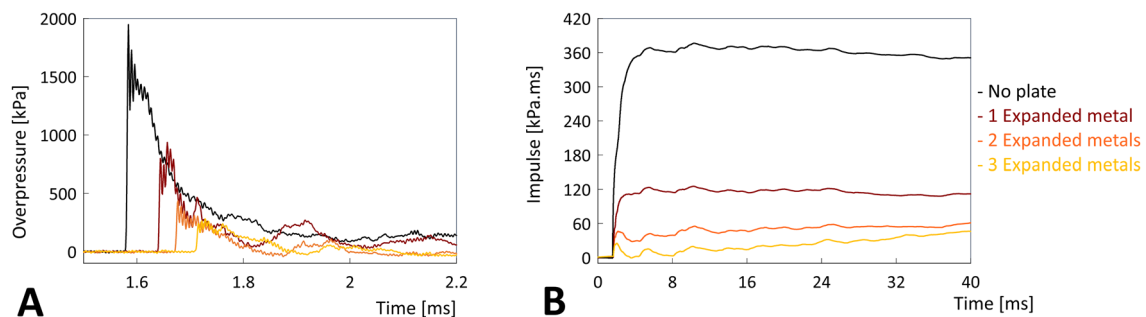

Fig. 12 Reflected overpressure (**A**) and impulse (**B**) measured on the wall positioned 50 mm behind two plates having either square or round holes, for two values of spacing. One reference test, which was performed without plates, is also shown

Fig. 13 Reflected overpressure (**A**) and impulse (**B**) measured on the wall positioned 50 mm behind one, two or three expanded metal plates. One reference test, which was performed without plates, is also shown

to be transmitted. Thus, the most influencing factor for the interaction is the plate porosity. These results are in line with previously published studies [8–10] performed with conventional shock tubes. Indeed, these studies show that the porosity has the greatest effect on overpressure reduction, whereas the geometry has almost no impact. The most fragile plates (the thinnest) were distorted after test but the damages had probably no effect on the attenuation of the blast wave. They occurred long after the passage of the wave on the gauge and so the measurement of the overpressure profile. In this work, we

have observed that an array of several plates or a 3D grid were more effective in mitigating the blast wave. This was to be expected as the initial shock wave is reflected several times and strongly disturbed before impacting the wall. It can be noted that in the case of two plates with square holes, the mitigation was fairly similar to the one obtained with one single plate. However, in the case of plates having a lower porosity, the mitigation increases with the number of plates. The fact that the shock wave trapping between several perforated plates enhances the shock wave attenuation downstream was already reported
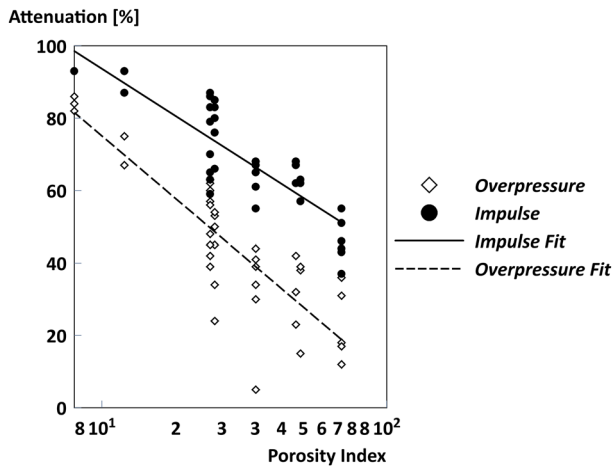
Fig. 14 Attenuation of the overpressure and of the impulse as a function of the porosity index (P/N) in a logarithmic scale. Overpressure fit: 141-29 ln(P/N); impulse fit: 141-21 ln(P/N)

in [17, 21]. In [21], a set of experiments was performed to investigate the effects of the number of plates placed in a given volume. The authors reported that the first plate determined the pressure build-up time and that, depending on the porosity of the perforated plates, the number of plates within the volume facilitated the attenuation of the incident shock wave and any further shock reverberations. Overall, these results have shown that similar phenomena of blast interaction with perforated plates occurred at low and high loading.

5 Conclusion

In this paper, we investigated the mitigation of a blast wave after its passage through one or several perforated plate(s). The use of an EDST allowed us to test the mitigation capacity of perforated plates under a high dynamic loading, and the use of a retroreflective shadowgraph technique with fast imaging allowed for a visualisation of the interaction. The results have shown that blast interaction with perforated plates at high loading is similar to what occurs at low loading. The overpressure and the impulse of the reflected blast wave on a wall located downstream from the plates(s) were assessed. We observed that an array of two or three plates was more effective in mitigating the blast wave. No effect on the blast mitigation was observed when the distance between two perforated plates varied. Among the different types of perforated plates tested, expanded metal and cast metallic foam seem to be valuable candidates for blast mitigation. Expanded metal is stronger than an equivalent weight of wire mesh, and has an interesting geometry enhancing the reflection of the shock wave along with a low porosity.

Downstream from two plates made of expanded metal, the reflected overpressure and impulse were strongly reduced. To the best of our knowledge, the blast mitigation capability of cast metallic foam was not yet investigated. The present work has shown that cast metallic foam was highly resistant to blast wave and its blast mitigation capacity was excellent.

Availability of data and materials Authors can confirm that all relevant data are included in the article and/or its supplementary information files.

Declaration

Conflict of interest The authors declare that there is no conflict of interest.

References

1. Catlin CA, Gregory CAJ, Johnson DM, Walker DG (1993) Explosion mitigation in offshore modules by general area deluge. TransIChem 71:101–111
2. Schunck T, Bastide M, Eckenfels D, Legendre JF (2020) Blast mitigation by water mist: the effect of detonation configuration. Shock Waves 30:629–644. https://doi.org/10.1007/s00193-020-00960-1
3. Blanc L, Sturtzer MO, Jung A, Diebels S, Kleine A (2019) Blast wave mitigation with galvanised polyurethane foam in a sandwich cladding. In: 32th International symposium on shock wave, Singapore
4. Berger S, Sadot O, Ben-Dor G (2010) Experimental investigation on the shock-wave load attenuation by geometrical means. Shock Waves 20:29–40. https://doi.org/10.1007/s00193-009-0237-3
5. Ben-Dor G, Britan A, Elperin T, Igra O, Jiang JP (1997) Experimental investigation of the interaction between weak shock waves and granular layers. Exp Fluids 22:432–443. https://doi.org/10.1007/s003480050069

6. Britan A, Ben-Dor G, Igra O, Shapiro H (2001) Shock waves attenuation by granular filters. Int J Multiphase flow 27:617–634. https://doi.org/10.1016/S0301-9322(00)00048-3

7. Dosanjh DS (1956) Interaction of grids with traveling shock waves. NACA TN 3680, John Hopkins University

8. Kingery C, Pearson R, Coulter G (1977) Shock wave attenuation by perforated plates with various hole sizes. USA Ballistic Research Laboratory Memorandum Report n° 2757

9. Britan A, Karpov AV, Vasilev EI, Igra O, Ben-Dor G, Shapiro E (2004) Experimental and numerical study of shock wave interaction with perforated plate. J Fluid Mech 126:399–409. https://doi.org/10.1115/1.1758264

10. Britan A, Igra O, Ben-Dor G, Shapiro E (2006) Shock wave attenuation by grids and orifice plates. Shock Waves 16:1–15. https://doi.org/10.1007/s00193-006-0019-0

11. Zare-Behtash H, Gongora-Orozco N, Kontis K, Jagadeesh G (2013) Detonation-driven shock wave interactions with perforated plates. Proc Inst Mech Eng Part G 228:671–678. https://doi.org/10.1177/0954410013478255

12. Schunck T, Bastide M, Eckenfels D, Legendre JF (2021) Explosion mitigation by metal grid with water curtain. Shock Waves. https://doi.org/10.1007/s00193-021-01004-y

13. Langdon GS, Nurick GN, Balden VH, Timmis RB (2008) Perforated plates as passive mitigation systems. Def Sci J 58:238–247. https://doi.org/10.14429/dsj.58.1644

14. Langdon GS, Rossiter IB, Balden VH, Nurick GN (2010) Performance of mild steel perforated plates as a blast wave mitigation technique: experimental and numerical investigation. Int J Impact Eng 37:1021–1036. https://doi.org/10.1016/j.ijimpeng.2010.06.001

15. Xiao W, Andrae A, Gebbeken N (2019) Experimental investigations of shock wave attenuation performance using protective barriers made of woven wire mesh. Int J Impact Eng 131:209–221. https://doi.org/10.1016/j.ijimpeng.2019.05.016

16. Gebbeken N, Rüdiger L, Warnstedt P (2018) Explosion mitigation by water mist-ring mesh with water curtain. In: 25th Military aspects of blast and shock conference, The Hague

17. Seeraj S (2007) Shock wave interactions with porous plates. Master degree thesis of the Faculty of Engineering University of the Witwatersrand, Johannesburg

18. Louar MA, Belkassem B, Ousji H, Spranghers K, Kakogiannis D, Pyl L, Vantomme J (2015) Explosive driven shock tube loading of aluminium plates: experimental study. Int J Impact Eng 86:111–123. https://doi.org/10.1016/j.ijimpeng.2015.07.013

19. Ousji H, Belkassem B, Louar MA, Reymen B, Martino J, Lecompte D, Pyl L, Vantomme J (2017) Air-blast response of sacrificial cladding using low density foams: experimental and analytical approach. Int J Mech Sci 128–129:459–474. https://doi.org/10.1016/j.ijmecsci.2017.05.024

20. Stojko S, Freundt J, Anderson JG, Delaney T (2018) Experimental characterization of the interaction of blast waves from multiple high explosive charges In: 25th Military aspects of blast and shock conference, The Hague

21. Ram O, Ben-Dor G, Sadot O (2018) On the pressure buildup behind an array of perforated plates impinged by a normal shock wave. Exp Therm Fluid Sci 92:211–221. https://doi.org/10.1016/j.expthermflusci.2017.11.014